THE JOURNAL OF PHYSICAL CHEMISTRY B

Article

pubs.acs.org/JPCB

A Novel Approach to the Investigation of Passive Molecular Permeation through Lipid Bilayers from Atomistic Simulations

Zhaleh Ghaemi,[†] Manuela Minozzi,[†] Paolo Carloni,[‡] and Alessandro Laio*[,†]

[†]SISSA- Scuola Internazionale Superiore di Studi Avanzati, via Bonomea 265, 34136 Trieste, Italy

[‡]Computational Biophysics, German Research School for Simulation Sciences, D-52425 Jülich, Germany and Institute for Advanced Simulation, Forschungszentrum Jülich, D-52425 Jülich, Germany

Supporting Information

ABSTRACT: Predicting the permeability coefficient (P) of drugs permeating through the cell membrane is of paramount importance in drug discovery. We here propose an approach for calculating P based on bias-exchange metadynamics. The approach allows constructing from atomistic simulations a model of permeation taking explicitly into account not only the "trivial" reaction coordinate, the position of the drug along the direction normal to the lipid membrane plane, but also other degrees of freedom, for example, the torsional angles of the permeating molecule, or variables describing its solvation/desolvation. This allows deriving an accurate picture of the permeation process, and constructing a detailed molecular model of the transition state, making a rational control of permeation properties possible. We benchmarked this approach on the permeation of ethanol molecules through a POPC membrane, showing that the value of P calculated with our model agrees with the one calculated by a long unbiased molecular dynamics of the same system.

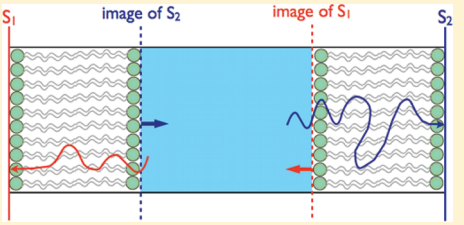

1. INTRODUCTION

In order to reach their targets, most drugs must cross at least one cellular membrane. Therefore, in drug discovery projects, understanding and controlling the process of permeation through the cell membrane is almost as important as improving the affinity toward the target. One of the important quantities to be optimized is the speed of permeation of the drugs through a membrane. This is measured by the permeability coefficient P, defined as the ratio of the flux through the membrane to the concentration difference across it. In some cases, drugs enter the cell exploiting transporters or channels.[1] However, the most common route of transport is *unassisted permeation* directly through the membrane as a consequence of the concentration gradient. Unassisted permeability coefficients can indirectly be determined in experiments by exploiting artificial membranes, such as unilamellar vesicles[2] or the so-called black lipid membranes.[3] One determines the value of P by measuring the change in concentration of the drug as a function of time in a chamber separated from another chamber by the membrane.[3] Automated procedures, such as parallel artificial membrane permeation assays (PAMPA), allow one to determine P quickly and reliably for several potential drugs.[4]

The permeability coefficient of a drug can also be estimated theoretically. Early attempts were based on Overton's observation, by which the permeability coefficient of a molecule is linearly correlated with its oil/water partition coefficient K.[5] In the so-called homogeneous solubility diffusion model, the membrane is modeled as a homogeneous slab of oil and the permeability coefficient P is estimated as $P = (K{\cdot}D)/h$, where D is the diffusion coefficient of the solute in oil and h is the thickness of the membrane.[6] Quantitative structure activity relationships (QSAR) allow one to estimate the permeability coefficient by an empirical equation whose parameters are trained by reproducing the observed P for a large data set of compounds.[7] Unfortunately, these approaches cannot provide hints for rational design of molecules with better permeability coefficient because of the lack of atomistic details. Moreover, they do not take into account the heterogeneity of the membrane. The latter plays an important role in drug permeation.[8]

To address these issues, the so-called inhomogeneous solubility diffusion model was developed.[9,10] This model relies on atomistic simulation-based free energy calculations, and estimates P as

$$\frac{1}{P} = \int_{z_1}^{z_2} \frac{dz}{D(z)} \exp[\beta \Delta F(z)] \tag{1}$$

where $F(z)$ is the free energy and $D(z)$ is the position dependent diffusion coefficient at position z along the direction normal to the lipid membrane plane. This equation is at the basis of most estimates of P from atomistic simulations.[11] The free energy, $F(z)$, can be computed with several techniques, for example, umbrella sampling, thermodynamic integration, and several other methods.[12−15] The position dependent diffusion coefficient is normally estimated by the z-constraint method.[10]

Special Issue: Macromolecular Systems Understood through Multi-scale and Enhanced Sampling Techniques

Received: February 2, 2012
Revised: April 25, 2012

   dx.doi.org/10.1021/jp301083h | J. Phys. Chem. B XXXX, XXX, XXX−XXX

Computing P by eq 1 involves describing the permeation process with only one degree of freedom, the value of z.[11,16,17] However, this degree of freedom alone might not be sufficient to describe the complex molecular processes leading to the partitioning of the molecule from aqueous solution and to its translocation through the membrane. For example, if the permeating molecule has a hydrophilic group, its coordinating water molecules have to be substituted by the aliphatic groups of the lipid tails. This process can in principle take place also at fixed z and can correspond to the rate limiting step of the permeation process. Other examples of degrees of freedom that can be critically coupled to z are the torsional dihedrals of the permeating molecule. Pharmacologically relevant molecules often exist in several conformers, and their most stable conformation in water solution can be different from the one taken during permeation. In other words, the value of z is not necessarily the correct reaction coordinate of the permeation process and more degrees of freedom have to be taken into account to describe the permeation appropriately. If one attempts to describe the dynamics of the system by z alone, the correct equation describing its evolution will necessarily have to include a kernel that decays slowly to zero,[18] making the numerical estimate of D in eq 1 difficult.

Here, we propose an approach that allows computing P, taking explicitly into account a large number of important slow degrees of freedom associated with the permeation process. We use bias-exchange metadynamics[19] as an enhanced sampling technique, to obtain an estimate of the multidimensional free energy surface as a function of several putative reaction coordinates. In this approach, including an extra reaction coordinate can only improve convergence. A subset of relevant coordinates sufficient to describe the process can be chosen afterward, with no extra computational cost. We then compute the position dependent diffusion matrix, using the procedure in ref 20. Finally, we perform a long kinetic Monte Carlo (KMC) simulation on a multidimensional model defined by the free energy and the diffusion matrix. KMC produces a realistic trajectory of the process on arbitrarily long time scales. The permeability coefficient is directly estimated from the dynamics, and permeation is observed "in real time", allowing an unbiased analysis of the molecular rearrangements on its basis. The faithfulness of the multidimensional kinetic model to the true dynamics can be verified by standard techniques, e.g., computing the diffusion matrix for different time lags. These calculations allow one to compute the mean value of the permeation times (MPT). The value of the permeability coefficient is then directly computed from the MPT.

We benchmark this approach on the permeation of ethanol through a membrane of palmitoyloleoylglycerophosphocholine (POPC) molecules. We show that the MPT for permeation of ethanol molecules computed based on our model falls within the error of the MPT computed by a long unbiased molecular dynamics (MD) simulation. The permeability coefficient of ethanol obtained by our protocol is compared with the experimental estimate by Ly and Longo.[21]

2. METHODS

2.1. Molecular Dynamics. We performed simulations on two systems with different sizes: a relatively larger system (LS) with 2 × 64 POPC molecules and a smaller system (SS) with 2 × 16 POPC molecules. For both systems, we used GAFF parameters for POPC lipids,[22] parameters from ref 23 for ethanol, and the TIP3P water model.[24] An equilibrated POPC lipid bilayer was kindly provided by T. A. Martinek with an area per lipid of 0.72 nm^2. The bilayer was placed in the $x-y$ plane of the simulation box. In both systems, ethanol molecules were randomly added to the simulation box and the rest of the box was filled with water molecules. In the case of the LS, the initial ethanol concentration in water is 1 mol %. Thus, LS (SS) contained 5953 (1628) water molecules and 60 (5) ethanol molecules in a volume of 6.15(3.66) × 7.56(3.14) × 7.59(7.96) nm^3. The lipid, water, and alcohol molecules were coupled to a heat bath at a temperature of 323 K, much above the POPC phase transition temperature,[25] using a Nose−Hoover thermostat[26,27] with a coupling constant of 1 ps. Pressure was controlled in the direction normal to the bilayer surface by a Parrinello−Rahman barostat[28] with a time constant of coupling of 1 ps. All the bonds were constrained to their equilibrium values by the LINCS algorithm.[29] Lennard-Jones interactions were cut off at a distance of 0.9 nm, and the time step was set to 2 fs. Long-range electrostatics were computed by the particle-mesh Ewald algorithm.[30] All simulations were performed by using the GROMACS package.[31]

2.2. Bias-Exchange Metadynamics. In bias-exchange metadynamics[19] (BE-META), several replicas of the system (walkers) are run in parallel biased with metadynamics history-dependent potentials acting on one collective variable (CV). To enhance the sampling, at fixed time intervals, bias potentials are exchanged between pairs of walkers which are selected at random with a probability of

$$\min\left\{1, \exp\left[\frac{1}{T}(V_G^a(x^a, t) + V_G^b(x^b, t) - V_G^a(x^b, t) - V_G^b(x^a, t))\right]\right\} \quad (2)$$

where $x^{a(b)}$ are the coordinates of walkers a (b) and $V_G^{a(b)}$ are the metadynamics potential acting on walker a (b).

In describing the permeation process, we are interested in describing the position of ethanol in the membrane as well as in discriminating contacts of ethanol with water molecules (W) and with groups of phospholipid molecules having different chemical nature, namely, the phosphate atoms of the head groups (P) and the aliphatic carbons of the tails of POPC molecules (T). For each ethanol molecule, we consider two centers denoted by O and C for oxidril and hydrophobic groups, respectively. Thus, the mechanism of permeation of ethanol molecules through the POPC membrane is modeled by the following seven collective variables: (1) the z component of the position vector connecting the center of mass of POPC molecules to the center of mass of an ethanol molecule and the coordination number of (2) O with P; (3) O with T; (4) O with W; (5) C with P; (6) C with T; and (7) C with W. The coordination number is estimated as

$$S = \sum_{i\in G_1}\sum_{j\in G_2} C(r_{ij}) \quad (3)$$

$$C(r_{ij}) = \frac{1 - \left(\frac{r_{ij}}{r_0}\right)^n}{1 - \left(\frac{r_{ij}}{r_0}\right)^m} \quad (4)$$

where r_{ij} is the distance between atoms i and j and sums run over the two appropriate sets of atoms (G_1 and G_2). For all the collective variables, we take r_0 = 0.25 nm, m = 4, and n = 2. The BE-META simulation was performed for a total time of 140 ns

dx.doi.org/10.1021/jp301083h | J. Phys. Chem. B XXXX, XXX, XXX−XXX

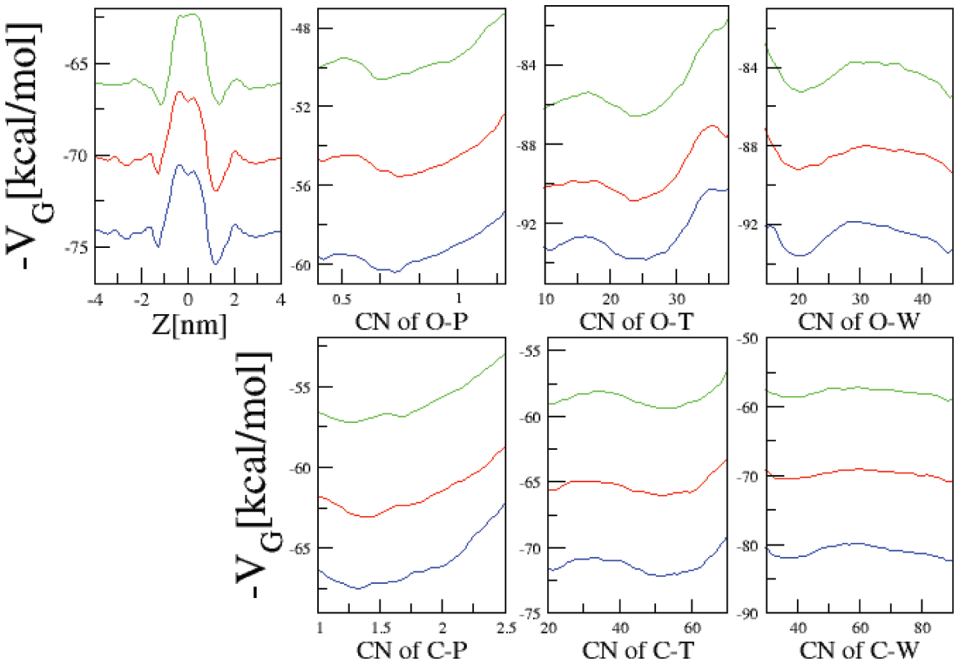

Figure 1. Evolution of the biasing potentials during simulation time. Each profile is a time average of the biasing potential: green profiles between 30 and 60 ns, red between 60 and 90 ns, and blue between 90 and 120 ns.

on seven walkers, biasing the described collective variables. The parameters for this simulation are as follows: Gaussian height is 0.072 kcal/mol and Gaussian widths are 0.2 nm for CV1, 0.03 for CV2, 1.3 for CV3 and CV4, 0.07 for CV5, 1.7 for CV6, and 2.0 for CV7 with a Gaussian deposition of every 5 ps and exchange attempts of every 20 ps. These values are chosen according to the criterion in ref 32. In Figure 1, the evolution of the biasing potentials for all collective variables is shown. Remarkably, the history-dependent potentials of metadynamics are very similar at different times, indicating that the choice of the collective variables is appropriate, and the system is capable of reaching convergence.[33,34]

2.3. Kinetic Model Construction. A thermodynamic and kinetic model was constructed on the basis of the BE-META results applying the protocol introduced in ref 20. First of all, the configurations explored by all the walkers are partitioned in hypercubes in CV space. The set of structures belonging to a hypercube play the role of a microstate in a discrete-state Markov model. In these microstates, the CV corresponding to the centers are equally spaced. This allows estimating the transition probability between two microstates by a simple equation (see below). Then, the equilibrium free energy of every microstate is estimated by applying a weighted histogram analysis method (WHAM).[35] Next, the transition rate matrix between the microstates is calculated by assuming that on a suitably long time scale the transitions between the microstates follow a Markov process. The transition rate between two microstates α and β is assumed to depend on the free energies (F_α and F_β) and the diffusion coefficient of the two microstates by

$$k_{\alpha\beta} = k^0_{\alpha\beta} \exp\left[-\frac{1}{2T}(F_\alpha - F_\beta)\right] \tag{5}$$

where T is the temperature and $k^0_{\alpha\beta} = k^0_{\beta\alpha}$ depends linearly on the diffusion matrix, D. The explicit expression of k^0 is given in ref 20.

Since lipid membranes are inhomogeneous systems, the diffusion matrixes are considered to be position dependent. Consistently with the topology of the free energy landscape (see Results and Discussion), we computed three diffusion matrixes, one for ethanol to be in water, one for ethanol coordinated by the lipid tails of POPC molecules, and one for ethanol hydrogen bonded under the surface of each leaflet (HB state in Results and Discussion).

The three matrixes were determined separately by using a maximum likelihood technique.[36,20] In this approach, one maximizes the likelihood that a given MD trajectory is reproduced by a trajectory generated based on the rate model in eq 5. To compute D, one generates a MD trajectory (or a set of trajectories) in the relevant region and maps it for a given time lag Δt on the microstates. Starting by an initial guess of D, several trajectories of the rate model are harvested starting from the microstates visited by MD and conditional probabilities for transitions among all the pairs of microstates are calculated. These probabilities are used to calculate a likelihood which is defined as

$$L(D) = \log \prod_t P_D(\alpha(t + \Delta t)|\alpha(t)) \tag{6}$$

that is then optimized as a function of D.[20] Practically an iterative line minimization is performed as a function of each matrix element. In this procedure, starting with an initial value and along a given direction, $L(D)$ is computed for 20 values of D and the matrix element value corresponding to the minimum of L is determined. Next, the procedure is repeated for other matrix elements and iterated until convergence. Since the calculated diffusion matrix depends on the time lag, if the rate model is well-defined, by increasing Δt, the matrix converges to a well-defined value. This is an indication that on a time scale larger than Δt the dynamics between microstates is approximately Markovian and the model in eq 5 faithfully describes the real dynamics of the system.

dx.doi.org/10.1021/jp301083h | J. Phys. Chem. B XXXX, XXX, XXX–XXX

2.4. Permeability Coefficient Calculation. We derive an equation that allows one to compute the permeability coefficient directly from a MD or a KMC simulation of the model eq 5. Consider a container separated from the outside by a membrane. In stationary conditions, the permeability coefficient is defined as the ratio between the flux J and the concentration difference ΔC across the membrane:

$$P = \frac{J}{\Delta C} \tag{7}$$

This equation cannot be used in a simulation setup like the one used in this work where, due to the periodic boundary conditions, the concentration difference across the membrane is by construction zero, and the flux through the membrane is also zero. In order to estimate P, we use instead the MD (or KMC) trajectory to estimate the total reactive flux through the membrane, without considering the direction of the molecules. Denoting by $J_{L\to R}$ (respectively $J_{R\to L}$) the flux from left to right (resp, from right to left), we estimate P as

$$P = \frac{J_{L\to R} + J_{R\to L}}{C} \tag{8}$$

where C is the ethanol concentration in water in stationary conditions. This equation is simply eq 7 written for a box of water enclosed on the right and on the left side by a membrane. Two surfaces S_1 and S_2 act as (virtual) sinks and sources of molecules as depicted in Figure 2. In particular, S_1, located

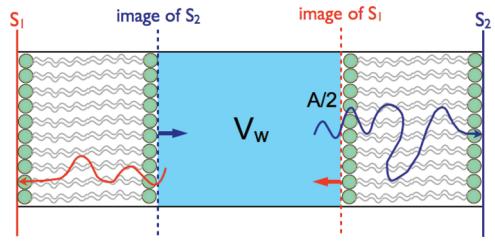

Figure 2. The box of water enclosed on both sides by a membrane. The adsorbing surfaces (S_1 and S_2) used in the derivation of eq 8 and their images are depicted. The red (resp blue) curved arrow represents a trajectory of a molecule contributing to the reactive flux $J_{R\to L}$ (resp $_{L\to R}$).

corresponding to lipid head groups on the left, acts as a sink for ethanol molecules coming from the right side of the membrane. S_2, located corresponding to head groups on the right, acts as a sink for ethanol molecules coming from the left. A molecule is classified as "coming from the right" and contributes to $J_{R\to L}$ if it reaches S_1 coming from the right side of the membrane, and not by looking at its velocity when it crosses the surface. With this choice, the currents in eq 8 are reactive currents, and not microscopic currents (much larger than the former due to recrossings). When an ethanol molecule crosses S_1 (and contributes to $J_{R\to L}$), it is virtually removed from the system. In order to keep the concentration "inside" the cell constant, one virtually adds a "new" ethanol molecule at the image of S_1 (resp S_2) for each molecule adsorbed by S_1 (resp S_2).

Denoting the volume of the simulation box occupied by water by V_w and the number of solvated ethanol molecules by N_w, C in eq 8 is estimated as $C = N_w/V_w$. The flux is instead estimated from the average time between two successive permeations $\bar{\tau}$, and from the total area of the membrane A:

$$J_{L\to R} + J_{R\to L} = \frac{1}{\bar{\tau}}\frac{1}{A}$$

Thus,

$$P = \frac{V_w}{N_w}\frac{1}{\bar{\tau}}\frac{1}{A} = \frac{1}{\bar{\tau}}\frac{L_w}{2N_w} \tag{9}$$

where L_w is the length of the simulation box in the z direction (normal to the membrane) that is occupied by water. The factor 2 in eq 9 arises from the fact that the efficacious area of the membrane is twice the area of the simulation box in the direction normal to z. Notice that the product between $\bar{\tau}$ and N_w appearing in eq 9 is approximately independent of N_w (it is exactly independent in the limit of small concentration). In particular, their product is estimated by the mean time between two successive permeations of a single molecule, denoted by MPT in the previous sections. Recapping, the permeability coefficient can be estimated in a MD run performed in a system with periodic boundary conditions, or in a rate model constructed as described in this work, as

$$P = \frac{L_w}{2\mathrm{MPT}} \tag{10}$$

where MPT is the average time between two successive permeations of a single molecule.

3. RESULTS AND DISCUSSION

3.1. Molecular Mechanism of Permeation. We performed a BE-META simulation[19] on a system of five ethanol molecules with a POPC membrane solvated by TIP3P water molecules. The simulation was performed for a total time of 140 ns on seven walkers, biasing variables that take into account the position of ethanol within the membrane and the type and number of contacts of ethanol with the water molecules and with the groups of POPC molecules having different chemical nature (see Methods for more details).

3.1.1. Microstate Determination and Free Energy Surface Construction. A careful analysis of the BE-META trajectories showed that an accurate description of thermodynamics and kinetics could be obtained by considering four CVs, the position of ethanol in the direction normal to the membrane (z), the coordination number of the oxidril group of ethanol (O) with aliphatic carbons of the tails of POPC (T), of the hydrophobic group of ethanol (C) with T, and of C with water molecules (W). These collective variables were defined in detail in Methods. BE-META trajectories were analyzed by subdividing the CV space of these four variables in hypercubic boxes (microstates) with a size of d_1 = 0.42 nm, d_2 = 10, d_3 = 19.5, and d_4 = 8. The free energy of each microstate in this CV space was determined applying the approach of ref 20.

In Figure 3, the free energy as an average of history dependent potentials of bias exchange metadynamics along z is depicted. The minimum of the free energy along this CV corresponds to ethanol in a state, hereafter denoted by HB state, where ethanol makes hydrogen bonds either with carbonyl or phosphate groups of POPC molecules. This state was also identified in ref 37. Two representative configurations of the HB state are shown in panels A and B of Figure 4, respectively. The two tiny barriers present at $z = \pm 0.24$ nm in Figure 3 correspond to the rate limiting step of the permeation process, associated with the transition between the HB state and a state in which ethanol is fully coordinated by the hydrophobic tails of POPC molecules. However, these barriers

dx.doi.org/10.1021/jp301083h | J. Phys. Chem. B XXXX, XXX, XXX−XXX

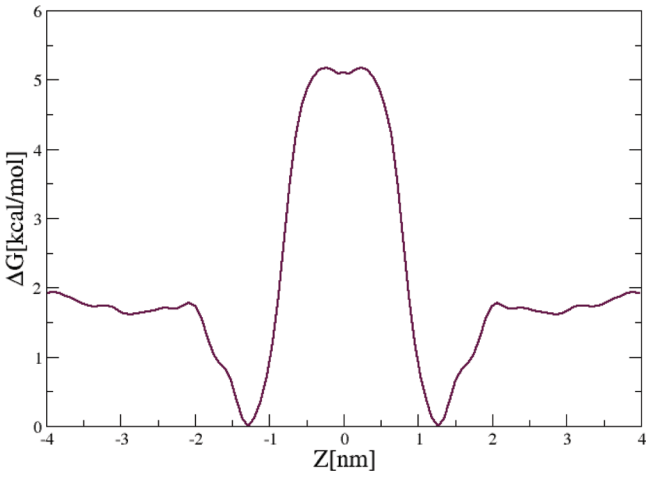

Figure 3. One-dimensional free energy as a function of z, the position of ethanol in the direction normal to the membrane. The free energy is obtained by averaging the history dependent potential of bias exchange metadynamics, also depicted in Figure 1.

are much smaller than k_BT, and the one-dimensional free energy landscape is basically characterized by a large transition region including all the values of z between −0.25 and 0.25 nm in which ethanol is surrounded by the hydrophobic tails of POPC, consistently with the homogeneous solubility diffusion model.[6]

The microstate corresponding to the transition state in the four-dimensional free energy landscape is characterized by a position of the ethanol within the membrane equal to 0, the coordination number of the oxidril group of ethanol (O) with the aliphatic carbons of the tails of POPC (T) and of the hydrophobic group of ethanol (C) with T have their maximum possible values and the coordination number of C with water molecules has its minimum possible value with respect to other states. This is consistent with the loss of hydrogen bonds to water molecules approaching this state, as suggested by structural insights obtained by our analysis. This state will be denoted as TS in the following. In the majority of the populated structures of TS, ethanol is in the middle of the membrane and has lost its hydrogen bond formed previously in the HB state. Instead, in few structures (0.3%), ethanol remains hydrogen bonded to a water molecule and drags it to the middle of the membrane, as depicted in Figure 5. The free energy difference between the solvated state of ethanol and TS is 3.5 ± 0.2 kcal/mol.

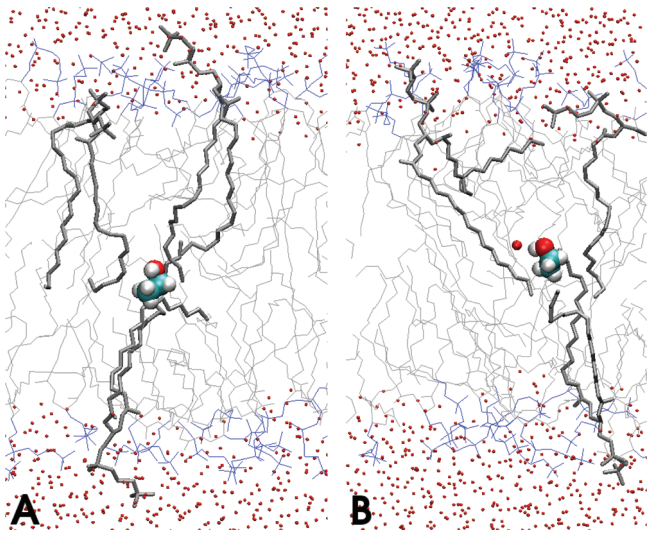

Figure 5. Ethanol in TS state: (A) permeating without any water molecule and (B) dragging a water molecule to the middle of the membrane. In both panels, the POPC molecules that are coordinating the ethanol are represented in licorice in gray, ethanol and water molecules in CPK, acyl chains of other POPC molecules in gray lines, and the rest of the POPC molecules in blue lines.

3.1.2. Position Dependent Diffusion Matrixes. To estimate the position dependent diffusion matrixes, we used the maximum likelihood approach introduced in refs 20 and 36 and described in Methods. We generated three different sets of MD trajectories in the relevant regions. A 40 ns trajectory for ethanol in water, a 50 ns trajectory in the HB state, and a 22 ns trajectory in the tail region. The trajectory in this region consisted of several short trajectories starting from the TS that were stopped as soon as ethanol exited from the region -1 nm $\leq z \leq 1$ nm. Assuming the matrixes are diagonal and a time lag of 70 ps, the following matrixes were obtained. For water region, $D_{11} = 7.5 \times 10^{-5}$ cm^2 s^{-1}, $D_{22} = 2.2$, $D_{33} = 8.5$, and $D_{44} = 2.6$; for HB region, $D_{11} = 2.5 \times 10^{-5}$ cm^2 s^{-1}, $D_{22} = 1.5$, $D_{33} = 220$, and $D_{44} = 1.2$; and for tail region, $D_{11} = 9.5 \times 10^{-6}$ cm^2

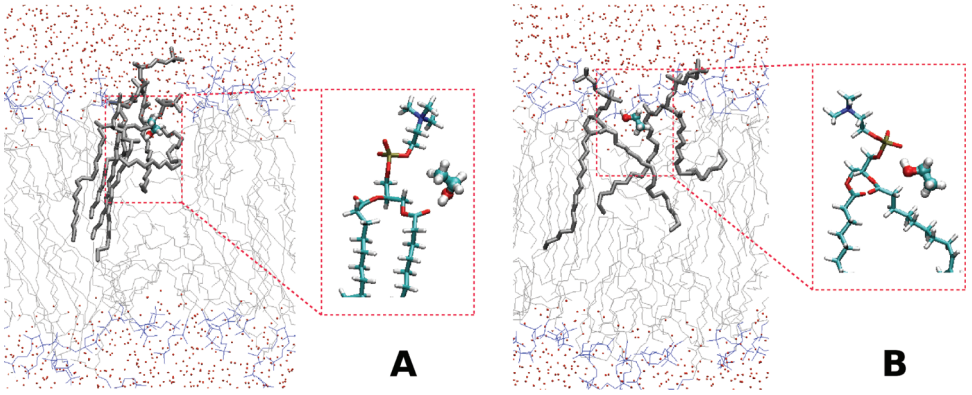

Figure 4. Representative configurations of ethanol in the HB state. (A) Ethanol forms hydrogen bonds with carbonyl groups of the acyl chains. (B) Ethanol forms hydrogen bonds with the phosphate groups. In both panels, POPC molecules coordinating ethanol are represented in licorice, ethanol in CPK, acyl chains of other POPC molecules in gray lines, and the rest of the POPC molecules in blue lines. A close-up view of the complexes is also shown.

dx.doi.org/10.1021/jp301083h | J. Phys. Chem. B XXXX, XXX, XXX−XXX

s^{-1}, D_{22} = 0.28, D_{33} = 1.25, and D_{44} = 1.2. To demonstrate the reliability of this calculation, in Figure 6, we report the values of

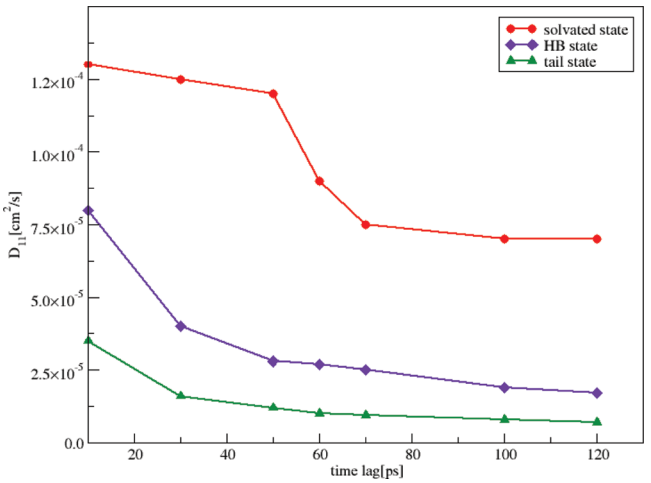

Figure 6. D_{11} in different regions estimated by maximum likelihood[20] from unbiased molecular dynamics trajectories as a function of the time lag.

D_{11} as a function of time lag for the three regions. The values reach a plateau for time lags equal or greater than 70 ps which shows that the rate model consistently reproduces the unbiased kinetics.[20]

3.1.3. Mean Permeation Time Estimation. In order to compute the mean permeation time of ethanol through the membrane (MPT), we generated a 5 ms KMC trajectory. To monitor permeations through the membrane, we assigned a direction to every ethanol, leaving the solvated state on one side. We count a transition when the ethanol reaches the solvated state on the other side. No transition is counted if ethanol bounces back to the side it has started from. The MPT is computed as the mean value of the time between two successive permeations. In Figure 7, we show the dependence

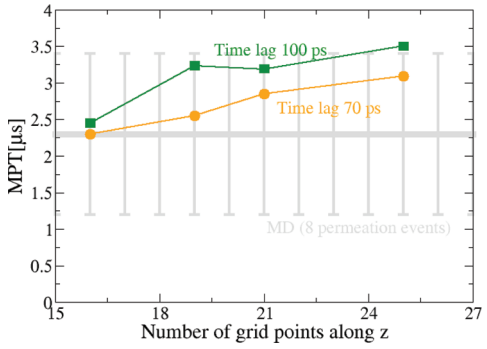

Figure 7. Dependence of MPT to the number of grid points used in the construction of the kinetic model, and on the time lag used for computing the diffusion matrix (see Figure 6). The gray region shows the MPT obtained by MD simulation.

of MPT on the number of grid points that were used for constructing the kinetic model, and for two different time lags. The estimate varies by a maximum of 30%, a remarkable accuracy for average transition times estimated by atomistic simulation. In order to verify if the MPT computed by the rate model is correct, we performed 300 ns of unbiased MD on the LS which contains 60 ethanol molecules on 128 POPC molecules. On this trajectory, positions of ethanol molecules in the simulation box versus time were monitored and successful permeations were counted with the same procedure applied for the rate model. In the simulation time, we observed eight successful permeations which by taking into account the number of ethanol molecules (60) gives the value of MPT as 2.3 ± 1.1 μs. This value is depicted in Figure 7 together with MPTs obtained by our model. Figure 7 shows that the MPT predicted by our model falls within the error of the MPT calculated from MD. This demonstrates that our approach allows estimating the MPT correctly.

3.2. Permeability Coefficient Calculation: Comparison of Unbiased MD Simulation and Experiment. Using our approach, we obtained values of permeability coefficient estimated based on unbiased MD as 8.5 ± 4.1 × 10^{-2} cm s^{-1} and based on the rate model as 6 × 10^{-2} cm s^{-1} (for a time lag of 70 ps and a number of grid points along z of 19).

We now compare our estimate with the permeability coefficient obtained by micropipet aspiration data.[21] In this experiment, an ethanol-free vesicle is placed in a constant flow of ethanol and the area expansion of the vesicle is monitored. A key assumption is that the more ethanol molecules get adsorbed at the bilayer the more the area of the vesicle expands. Through a series of equations, the adsorbed ethanol surface density and the ethanol concentration inside the vesicle are determined in order to model the area expansion. The permeability coefficient is estimated as the slope of the plot of the change of concentration of ethanol inside the vesicle versus time as 3.8 ± 3.0 × 10^{-5} cm s^{-1}. This value is 3 orders of magnitude smaller than what we found. The MPTs reported in the literature for ethanol−POPC or similar membrane systems are between 130 and 170 ns,[38,39] which shows an even faster permeation through the membrane than ours.

In order to investigate the origin of this discrepancy, we first attempted to describe the permeation process by a homogeneous solubility diffusion model.[6] As mentioned in the introduction, P is estimated in this approach as $P = (K{\cdot}D)/h$, where K is the oil/water partition coefficient, D is the diffusion coefficient, and h is the membrane thickness. The partition coefficient of ethanol estimated on the free energy surface obtained by our calculation is equal to 6.5 × 10^{-3}, which is consistent with the experimental value.[40] By setting the experimental values of P, K, and of the membrane thickness in the above equation, the diffusion coefficient turns out to be of the order of 10^{-8} cm^2 s^{-1}. However, the diffusion coefficient of ethanol in water is of the order of 10^{-5} cm^2 s^{-1}. Thus, according to this estimate, ethanol should diffuse in lipid tails approximately 1000 times slower than in water. This large difference seems rather unlikely, as for most of the solutes with roughly the same size of ethanol computational estimate of the diffusion coefficients show at most a difference of 1 order of magnitude,[11,17] although such calculations could be affected by systematic errors such as inaccuracy of force field.

Another possible reason for the observed discrepancy might be the specific approach used in the experiment, in which P is estimated from the area expansion of a vesicle as a function of time. Clearly, the volume of the vesicle becomes stable when the concentrations inside and outside are equal, and the change in volume is related to the permeability of the membrane. However, in order to reach stationary conditions, ethanol molecules must not only cross the membrane but also diffuse inside the vesicle. In order to quantify this effect, we computed the relaxation time of ethanol concentration at the center of a

dx.doi.org/10.1021/jp301083h | J. Phys. Chem. B XXXX, XXX, XXX−XXX

vesicle using eq 5 in the Supporting Information. We considered the experimental conditions for target ethanol concentration, c = 1.7 M and a vesicle radius ranging from R = 10 to 20 μm. This relaxation time is the time scale of the diffusion of ethanol molecules in water until the concentration reaches equilibrium. Considering the range of the radius of the vesicle, the relaxation time ranges between 0.78 and 3.13 s. From the experimental graphs (see Figure 17-A in ref 21), it is deduced that vesicle size gets equilibrated in a time scale of seconds which is consistent with our derived time scale for ethanol diffusion in the vesicle. Of course, these data do not exclude a permeation time through the membrane to be of the order of a fraction of seconds, as implied by the experimental value of P. However, our calculations indicate that in order to find out if this is the case one should repeat the experiment with much smaller vesicles.

4. CONCLUSIONS

One of the key factors that has to be addressed in order to rationally design a drug is its capability of crossing the cell membrane, quantified by the permeability coefficient, P. Since experimental techniques for measuring P are expensive and time-consuming, predicting the value of this coefficient by computer simulations is of paramount practical importance. The state-of-the-art computational approach for computing P is the inhomogeneous solubility diffusion model,[9,10] in which permeation is modeled by only one degree of freedom, the position of the permeating molecule in the direction normal to the membrane, z.[11,16,17] However, in pharmacologically relevant molecules, other degrees of freedom might be essential for describing accurately the permeation process, for example, the torsional degrees of freedom of the permeating molecule, or variables describing its solvation/desolvation. Neglecting these variables leads to a slowly decaying memory kernel in the dynamics of z,[18] making the numerical estimate of the diffusion coefficient in eq 1 difficult.

To illustrate this effect, we performed two MD simulations on a system consisting of 5 ethanol and 32 POPC molecules in aqueous solution. In the first simulation, we follow the procedure of ref 10 to compute $D(z)$; namely, we constrain the position of one ethanol in the middle of the membrane (at z = 0), and we compute the force autocorrelation function. In the second simulation, we compute the same correlation function but restraining also the values of the other three collective variables used for constructing the kinetic model. In Figure 8, we show the force correlation functions of the two simulations. In the simulation in which four collective variables are fixed, the correlation function decays to zero in a few ps. Instead, if one fixes only the value of z, important memory effects appear, with a relaxation time of at least 30 ps.

In addition to this effect (and maybe more importantly), describing permeation by a single variable may spoil the complexity of the molecular mechanism of permeation, making difficult a rational improvement of the permeability properties based on simulation results.

In this work, we propose a new approach to calculate P that allows addressing this issue, constructing a model of permeation in as many variables as necessary. Using bias-exchange metadynamics[19] and the approach of ref 20, we construct a multidimensional rate model taking into account several degrees of freedom, including z, and other putatively "slow" variables, for instance, the ones describing desolvation of the permeating molecule. Using this model, we compute the mean time of a permeation through the membrane (MPT). We derive a formula to compute P in simulations where the presence of periodic boundary conditions makes the flux and concentration difference across the membrane equal to zero. We show that P is directly related to the MPT, which can be computed directly from the rate model. This approach has been benchmarked on a system of 5 ethanol and 32 POPC molecules. We constructed a rate model in the space of four variables, the position of ethanol in the direction normal to the membrane, the coordination number of the oxidril group of ethanol (O) with aliphatic carbons of the tails of POPC (T), of the hydrophobic group of ethanol (C) with T, and of C with water molecules (W). Using this model, we estimated a permeability coefficient of 6×10^{-2} cm s^{-1}. In order to benchmark our approach, we also computed P by unbiased molecular dynamics on a system of 60 ethanol and 128 POPC molecules. We observed eight permeations, which led to an estimated value of P of $(8.5 \pm 4.1) \times 10^{-2}$ cm s^{-1}, consistent with the prediction of our model.

Even if this benchmark demonstrates that our approach can predict the value of P with excellent accuracy, our calculated value is 3 orders of magnitude larger than the one reported in ref 21, pointing to a possible systematic error due to the force field. However, in the experiment described in ref 21, P is measured indirectly, from the area expansion of an ethanol-free vesicle subject to a constant flow of ethanol molecules. It is correctly assumed that the vesicle area becomes stable when the ethanol molecule concentration inside and outside of the membrane is in equilibrium. However, the concentration of ethanol reaches equilibrium not only by permeation through the membrane but also by diffusion inside the vesicle. We show that the time scale of ethanol diffusion is of the order of seconds in the experimental conditions. This is very close to the relaxation time of vesicle area measured in experiments. This makes the interpretation of experimental results difficult, as one is not sure if the rate limiting step is membrane permeation or diffusion in the vesicle.

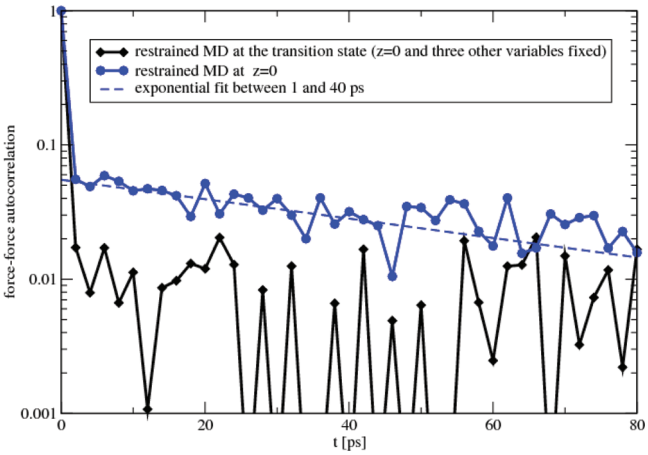

Figure 8. Force autocorrelation functions for an ethanol in the middle of the membrane (z = 0). Blue line with circles: only the value of z is fixed at z = 0. Blue dashed line: exponential fit to this autocorrelation function, between 1 and 40 ps. The estimated relaxation time is 62.6 ps. Black line with diamonds: the value of z is fixed at z = 0, and the values of the coordination number of the oxidril group of ethanol (O) with the aliphatic carbons of the tails of POPC (T), of the hydrophobic group of ethanol (C) with T, and of C with the water molecules are restrained to their values at TS.

dx.doi.org/10.1021/jp301083h | J. Phys. Chem. B XXXX, XXX, XXX−XXX

In conclusion, the results of this work demonstrate that the approach we present allows one to obtain values of P consistent with unbiased molecular dynamics, performed with the same force field. The test system (ethanol) has been chosen exactly because it permeates relatively quickly through a POPC membrane, allowing a direct benchmark of our approach. We plan to apply the same method for describing the permeation process and computing P of pharmacologically relevant molecules, in which it would be hopeless observing a permeation by brute force simulation.

■ ASSOCIATED CONTENT

Supporting Information

Further information is provided on relaxation time for concentration in a vesicle. This material is available free of charge via the Internet at http://pubs.acs.org.

■ AUTHOR INFORMATION

Corresponding Author

*E-mail: laio@sissa.it.

Notes

The authors declare no competing financial interest.

■ REFERENCES

(1) Alberts, B.; Johnson, A.; Lewis, J.; Raff, M.; Roberts, K.; Walter, P. *Molecular biology of the cell*, 4th ed.; Garland Science: New York, 2002.
(2) Paula, S.; Volkov, A.; Van Hoek, A.; Haines, T.; Deamer, D. *Biophys. J.* **1996**, *70*, 339−348.
(3) Xiang, T.-x.; Chen, X.; Anderson, B. D. *Biophys. J.* **1992**, *63*, 78−88.
(4) Kansy, M.; Senner, F.; Gubernator, K. *J. Med. Chem.* **1998**, *41*, 1007−1010.
(5) Overton, E. *Vierteljahrsschr. Naturforsch. Ges. Zuerich* **1896**, *41*, 383.
(6) Finkelstein, A. *J. Gen. Physiol.* **1976**, *68*, 127−135.
(7) Hansch, C.; Fujita, T. *J. Am. Chem. Soc.* **1964**, *86*, 1616−1626.
(8) Xiang, T.; Anderson, B. D. *Adv. Drug Delivery Rev.* **2006**, *58*, 1357−1378.
(9) Diamond, J. M.; Szabo, G.; Katz, Y. *J. Membr. Biol.* **1974**, *17*, 148−152.
(10) Marrink, S.; Berendsen, H. *J. Phys. Chem.* **1994**, *98*, 4155−4168.
(11) Marrink, S. J.; Berendsen, H. J. C. *J. Phys. Chem.* **1996**, *100*, 16729−16738.
(12) Widom, B. J. *J. Comput. Phys.* **1963**, *39*, 2808−2812.
(13) Koubi, L.; Tarek, M.; Klein, M. L.; Scharf, D. *Biophys. J.* **2000**, *78*, 800−811.
(14) Torrie, G. M.; Valleau, J. P. *J. Comput. Phys.* **1977**, *23*, 178−199.
(15) Shinoda, W.; Mikami, M.; Baba, T.; Hato, M. *J. Phys. Chem. B* **2004**, *108*, 9346−9356.
(16) Boggara, M. B.; Krishnamoorti, R. *Biophys. J.* **2010**, *98*, 586−595.
(17) Bemporad, D.; Essex, J. W.; Luttmann, C. *J. Phys. Chem. B* **2004**, *108*, 4875−4884.
(18) Risken, H. *The Fokker-Planck Equation: Methods of Solutions and Applications*, 3rd ed.; Springer-Verlag: Berlin, 1996.
(19) Piana, S.; Laio, A. *J. Phys. Chem. B* **2007**, *111*, 4553−4559.
(20) Marinelli, F.; Pietrucci, F.; Laio, A.; Piana, S. *PLoS Comput. Biol.* **2009**, *5*, No. e1000452.
(21) Ly, V.; Longo, M. L. *Biophys. J.* **2004**, *87*, 1013−1033.
(22) Jojart, B.; Martinek, T. A. *J. Comput. Chem.* **2007**, *28*, 2051−2058.
(23) Fox, T.; Kollman, P. A. *J. Phys. Chem. B* **1998**, *102*, 8070−8079.
(24) Jorgensen, W. L.; D., M. J. *J. Am. Chem. Soc.* **1983**, *105*, 1407−1413.
(25) Epand, R.; Bottega, R. *Biochim. Biophys. Acta* **1988**, *944*, 144−154.
(26) Nose, S. *Mol. Phys.* **1984**, *52*, 255−268.
(27) Hoover, W. G. *Phys. Rev. A* **1985**, *31*, 1695−1697.
(28) Parrinello, M.; Rahman, A. *J. Appl. Phys.* **1981**, *52*, 7182−7190.
(29) Hess, B.; Bekker, H.; Berendsen, H. J. C.; Fraaije, J. G. E. M. *J. Comput. Chem.* **1997**, *18*, 1463−1472.
(30) Darden, T.; York, D.; Pedersen, L. *J. Comput. Phys.* **1993**, *98*, 10089−10092.
(31) Lindahl, E.; Hess, B.; van der Spoel, D. *J. Mol. Model.* **2001**, *7*, 306−317.
(32) Cossio, P.; Marinelli, F.; Laio, A.; Pietrucci, F. *J. Phys. Chem. B* **2010**, *114*, 3259−3265 (PMID: 20163137).
(33) Laio, A.; Gervasio, F. L. *Rep. Prog. Phys.* **2008**, *71*, 126601.
(34) Crespo, Y.; Marinelli, F.; Pietrucci, F.; Laio, A. *Phys. Rev. E* **2010**, *81*, 4.
(35) Kumar, S.; Rosenberg, J. M.; Bouzida, D.; Swendsen, R. H.; Kollman, P. A. *J. Comput. Chem.* **1995**, *16*, 1339−1350.
(36) Hummer, G. *New J. Phys.* **2005**, *7*, 34.
(37) Feller, S. E.; Brown, C. A.; Nizza, D. T.; Gawrisch, K. *Biophys. J.* **2002**, *82*, 1396−1404.
(38) Patra, M.; Salonen, E.; Terama, E.; Vattulainen, I.; Faller, R.; Lee, B. W.; Holopainen, J.; Karttunen, M. *Biophys. J.* **2006**, *90*, 1121−1135.
(39) Terama, E.; Ollila, O. H. S.; Salonen, E.; Rowat, A. C.; Trandum, C.; Westh, P.; Patra, M.; Karttunen, M.; Vattulainen, I. *J. Phys. Chem. B* **2008**, *112*, 4131−4139.
(40) Stein, W. D. *Transport and Diffusion Across Cell Membranes*; Academic Press: New York, 1986.